Journal of Materials Chemistry B

Accepted Manuscript

ROYAL SOCIETY OF CHEMISTRY

www.rsc.org/materialsB

Journal Name

ARTICLE

Poly-(allylamine hydrochloride) but not poly(acrylic acid)-coated upconversion nanoparticles induce autophagy and apoptosis in human blood cancer cells

Received 00th January 20xx,

Accepted 00th January 20xx

DOI: 10.1039/x0xx00000x

www.rsc.org/

Jiaxiang Juan[a,#], Liang Cheng [b,#,§], Min Shi[a,#], Zhuang Liu[b], Xinliang Mao[a,c,§]

Upconversion nanoparticles (UCNPs) have gained increased attention due to its various medical applications such as drug delivery, detection, imaging, and photodynamic therapy. But little is known about its direct biological activity. In the present study, we synthesized $NaYF_4$:Yb,Er UCNPs coating with poly-(allylamine hydrochloride) (PAH) or poly(acrylic acid) (PAA) and investigated their effects in human myeloma and leukemia cells. When human myeloma and leukemia cells were incubated with both types of UCNPs, we found that PAH- but not PAA-UCNPs increased the expression of LC3-II, a hallmark of autophagy. This effect was confirmed by the accumulation of LC3 puncta analyzed by immunofluorescence microscopy. Induction of LC3-II could be blocked by 3-methyl adenosine (3-MA), an autophagy inhibitor. Consistent with this observation, PAH-UCNPs also inhibited both AKT and mTOR activation, the key step in autophagy activation. Further studies demonstrated that PAH-UCNPs also decreased Bcl-2 but increased Beclin1 and Atg14 expression, further suggesting PAH-UCNPs-induced autophagy was associated with increased activity of the PI3KC3/Beclin1 activity. Moreover, PAH-UCNPs induced apoptosis in myeloma cells and enhanced apoptosis induced by bortezomib and doxorubicin, two major anti-myeloma drugs. Therefore, our study suggested that PAH-UCNPs alone can induce both apoptosis and autophagy in human blood cancer cells by modulating the AKT/mTOR and the PI3KC3/Beclin1/Atg14 signaling pathways. This study implies the potential application of PAH-UCNPs in blood cancer-cell killing.

Introduction

Upconversion nanoparticles (UCNPs) are a new class of luminescent materials by doping rare earth elements including the lanthanoids, yttrium, and scandium. In the past few years, these UCNPs were widely used in the fields of traditional agriculture, industry, national defense, and high technology[1-7]. Because of excellent biocompatibility, photosensitivity, and deep penetrating near-infrared (NIR) light excitable upconversibility, UCNPs hold promising biomedical applications, including living imaging for cancer diagnosis, bio-probes to detect disease biomarkers, drug delivery system, and photodynamic therapy (PDT) in cancer therapy [2, 8-11]. UCNPs-coupled PDT has been shown great potential in the treatment of solid tumors due to its ability to penetrate thick tissue and to accumulate in specific tumor tissues [12-14] and has been tested in several cancer models, including liver cancer [15] and murine bladder cancer [16] . A recent study showed that silica-coated UCNPs can, in addition to tumor imaging, activate a platinum prodrug and display cytotoxicity against cisplatin-resistant ovarian carcinoma cells [17].

Autophagy is a protective cellular response to chemical, physical or biological stresses [18]. In the case of energy deprival, cells can initiate autophagy by degrading long-lived proteins as well as damaged organelles and recycling the nutrient substance to survive [18]. A variety of nanoparticles have been shown to induce autophagy which usually protects cell from stress insults or cell death. For example, iron oxide nanoparticles can induce pro-survival autophagy in both leukemia and myeloma cells [19]. Silver nanoparticles also induce cytoprotective autophagy in melanoma cells [20]. It is also reported that nanoparticles can induce pro-death autophay. Acute exposure to zinc oxide nanoparticles induces autophagic immune cell death [21]. Cerium dioxide nanoparticles induce autophagy and increase cytotoxicity of human monocytes [22]. But little is known about the effects of UCNPs on autophagy, one of the most important cell responses to chemical, physical or biological exposures. In the present study, we used high temperature to synthesize UCNPs and then modified these nanoparticles with poly(acrylic acid) (PAA-UCNPs) and poly-(allylamine hydrochloride) (PAH-UCNPs), which showed great potential in image diagnosis and PDT. To our surprise, PAH- but not PAA- modified UCNPs induced both autophagy and apoptosis. The study demonstrated that coating materials play a major role in the biological activities of UCNPs.

Methods

Chemicals

[a] *Jiangsu Key Laboratory of Translational Research and Therapy for Neuro-psycho-diseases, Department of Pharmacology, College of Pharmaceutical Sciences, Soochow University.Suzhou, China, 215123. E-mail: xinliangmao@suda.edu.cn; Tel: +86 512 65882152*
[b] *Institute of Functional Nano & Soft Materials Laboratory (FUNSOM), Jiangsu Key Laboratory for Carbon-Based Functional Materials & Devices, Collaborative Innovation Center of Suzhou Nano Science and Technology, Soochow University, Suzhou, China, 215123. Email: lcheng2@suda.edu.cn*
[c] *Jiangsu Key Laboratory of Preventive and Translational Medicine for Geriatric Diseases, Soochow University, China*
[#] *These authors contributed equally to this study*

All chemicals involved in this study were analytical grade and used without further purification. Y_2O_3, Yb_2O_3, and Er_2O_3 were purchased from Shanghai Chemical Industrial Co. All the rare-earth trifluoroacetates were prepared by dissolving the respective rare-earth oxides in trifluoroacetic acid (CF_3COOH, Shanghai Chemical Industrial Co.). Oleic acid (OA, 90%), Oleyl amine (OM) and 1-Octadecene (ODE >90%) were purchased from Sigma-Aldrich. Bortezomib (BZ) was purchased from Santa Cruz. Doxorubicin (Dox), dexamethasone (Dex), Bafilomycin A1 (BafA), and 3-methyladenine (3-MA) were purchased from Sigma-Aldrich.

Synthesis of UCNPs

In a typical procedure: 1 mmol of Re $(CF_3COO)_3$ (Y: Yb: Er = 69%: 30%: 1%), 2 mmol of CF_3COONa and 20 mL of solvent (10 mL OA /10 mL ODE) were brought to a 100-ml three-necked flask simultaneously and degassed at 140 °C for 30 min under vacuum. In the presence of nitrogen, the mixture was rapidly heated to 330 °C and kept at this temperature for 1 h under vigorous magnetic stirring. After cooling down to the room temperature, the product was precipitated by addition of ethanol, separated by centrifugation, and washed repeatedly by ethanol and water. The yielded nanoparticles could be re-dispersed in various non-polar organic solvents.

PAA coating on UCNPs

Coating of PAA on UCNPs was carried out following a literature protocol[23]. Poly (acrylic acid) (PAA MW=1800) (300 mg) was added into 30 mL diethylene glycol (DEG) in a three neck flask, and the mixture was heated to 110 °C to form a clear solution. Toluene solution (5 mL) containing 100 mg UCNPs was added slowly into the PAA solution with the temperature maintained for 1 h under nitrogen protection. The solution was then heated to 240 °C for 1 h. After cooling down to room temperature, the resultant solution wasadded ethanol to yield a precipitate. The PAA-UCNPs were recovered via centrifugation and washed several times with ethanol/water (1:1 v/v).

PAH coating on the PAA-UCNPs to generate PAH-UCNPs

PAA-UCNP solution (0.5 mg/mL, 5 mL) was dropwise added into 5 mL of PAH solution (MW=15000, 1 mg/mL) under ultrasonication for 30 min. After stirring for 4 h, a PAH- UCNP solution was obtained and purified by filtration through 100 kDa molecular weight cut off (MWCO) filters (Millipore) to remove excess PAH.

Characterization of UCNPs

Transmission electron microscopy (TEM, FEI Tecnai F20, acceleration voltage=200 KV) was applied to characterize the shape and size of UCNPs. X-ray diffraction (PANalytical X-ray diffractometer) equipped with Cuka radiation λ=0.15406 nm) was used to acquire the information of crystallography and phase of as-prepared UCNPs. Fourier transform Infra-red (FT-IR) spectrums were obtained by HYPERION (German, Bruker) from 4000 cm^{-1} to 400 cm^{-1}. Thermogravimetric–differential thermal analysis (TG–DTA) measurements of the products were performed using a Setaram TGA 92 instrument in the temperature range from room temperature to 500 °C at a heating rate of 10 °C/min.The sizes and zeta potentials of PAA- and PAH- coated UCNPs were measured with a Malvern zetasizer (ZEN3690, Malvern, UK). Concentrations of Y were measured by inductively coupled plasma atomic emission spectroscopy (ICP-AES).

Cell culture

Human multiple myeloma (MM) cell lines (OPM2 and JJN3) and leukemia cell lines (K562) were cultured in Iscove's modified Dulbecco's medium and RPMI-1640 media (HyClone), respectively. All media were supplemented with 10% fetal bovine serum (Gibco), 100 units/mL of penicillin and 100 μg/mL of streptomycin.

Antibodies

Specific antibodies against LC3, Beclin1, p62, Bcl-2, poly ADP-ribose polymerase (PARP), Caspase-3, mammalian target of rapamycin (mTOR), phosphorylated mammalian target of rapamycin (p-mTOR), protein kinase B (AKT), and phosphorylated protein kinase B (p-AKT) were purchased from Cell signaling Technologies, Inc. (Danvers, MA). Anti-glyceraldehyde-phosphate dehydrogenase (GAPDH) monoclonal antibody was purchased from Sigma (St. Louis, MO). Atg14 was purchased from Medical & Biological Laboratories Co., Ltd (Tokyo, Japan). Enhanced chemoluminescence (ECL) detection system and diamidino-phenyl-indole (DAPI) were provided by Beyotime Institute of Biotechnology, Nantong, China.

***In vitro* cytotoxicity assay**

OPM2 cells were seeded in 96-well plates at a density of 10^4 cells per well and cultured at 37 °C overnight. Then, the cells were added with PAA- and PAH- modified UCNPs solutions, respectively, with different concentrations and then incubated for 24 h. Trypan blue exclusion staining buffer was added to each well to stain the cells, and then blue cells were counted as dead cells.

Cell internalization of PAA- and PAH-UCNPs

Internalization of PAA- and PAH-UCNPs by cells was measured with ICP-AES. OPM2 (10^5) cells were seeded in 12-well plates and were incubated overnight at 37°C with equal amount of PAA-UCNPs or PAH-UCNPs. After incubation for various periods (0, 1, 2, 4, 8, 12, or 24 h), cells were collected and washed with PBS for two times before being boiled in aqua regia. Afterwards, the concentration of Y in each sample, which was diluted into 10 ml by water, was measured by ICP-AES.

Immunoblotting

Equal amount (30 μg) of total proteins were subjected to sodium dodecyl sulfate–polyacrylamide gel (SDS-PAGE) electrophoresis, followed by transfer to polyvinylidene difluoride membranes. The blots were then blocked with 5% non-fat milk for 1 h before being incubated with specific primary antibodies overnight at 4°C. Secondary antibody incubation and detection of the protein signals were performed as described previously [24].

Immunofluorescence

OPM2 cells (2.5×10^5) were plated in 12-well-plates and were treated with 100 μg/mL of PAH- or PAA- UCNPs for 9 h. Starvation and dimethyl sulfoxide (DMSO) treatment were used as a positive and negative control, respectively. OPM2 cells were then collected in cold phosphate buffer solution (PBS) and transferred to glass

slides using Cytospin by a centrifuge at 800 rpm for 5 min. Cells were then applied for Immunofluorescence analysis by staining with an anti-LC3 antibody using a protocol as described previously [25]. Before being analyzed on a confocal microscopy (Olympus), cells were incubated with DAPI for 10 min.

Studies in primary blood cells

Whole blood samples were collected in heparin-treated tubes from adult male mice (8 weeks old, 20-22 g, provided by Shanghai Slac Laboratory Animal Co. Ltd., Shanghai, China) were anaesthetized by an injection of 4% chloral hydrate. Nucleated cells were then isolated from whole blood samples by a gradient centrifugation using a Ficoll agent (Sigma-Aldrich), and subjected to incubation with PAH- or PAA- UCNPs for 9 h before being analyzed for the expression of LC3, Beclin1, Bcl-2 and GAPDH with specific antibodies. This study on mice was consistent with the Guide of Experimental Animal of Soochow University and it was approved by the Review Board for Animal Care and Welfare of Soochow University.

Results

Surface modification and characterization of UCNPs.

Yb and Er doped $NaYF_4$ UCNPs (Y : Yb: Er= 69% : 30% : 1%) were synthesized following a literature procedure with slight modifications[8]. An X-ray diffraction (XRD) analysis showed that hexagonal $NaYF_4$: Yb, Er nanocrystals with high purity were obtained (Fig. 1A). The as-prepared UCNPs were capped by oleic acid and were not water soluble. PAA polymers were used to transfer hydrophobic UCNPs into the aqueous phase, yielding PAA-UCNPs with excellent water solubility (Fig. 1B). After that, the cationic polymer PAH with a molecular weight (MW) of 15 KDa was applied to modify the surface of the PAA-UCNPs by electrostatic interaction. The successful PAH and PAA coating on the surface of UCNPs were determined by FT-IR spectroscopy (Fig. 1C) and thermogravimetric analysis (TGA, Fig. 1D). PAA- and PAH- coated UCNPs were negative and positive charged (Fig. 1E). Both PAA- and PAH- coated UCNPs were monodispersed with an average diameter of approximately 110 nm (Fig. 1F). The sizes of nanoparticles measured by dynamic light scattering (DLS) also slightly increased (Fig. 1F), showing an average hydrodynamic diameter of ~160 nm for the final product PAH-UNCPs.

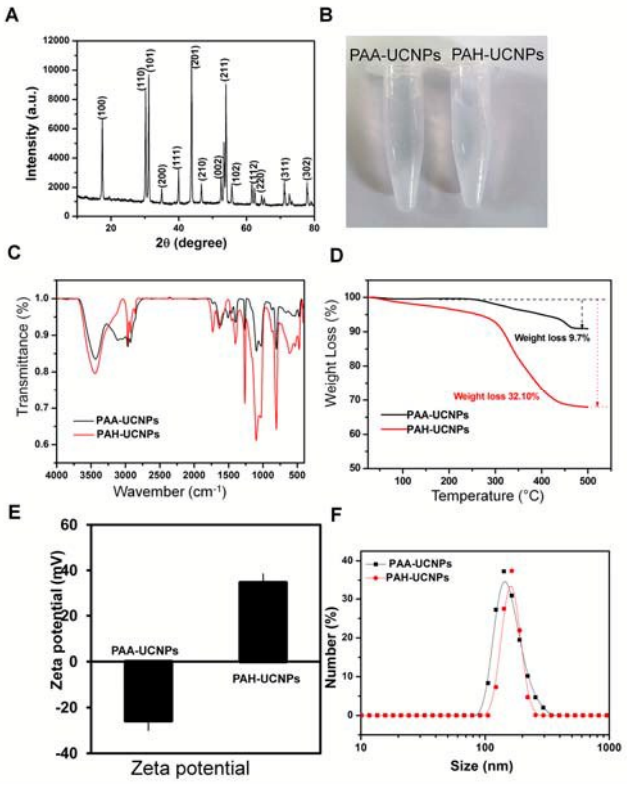

Fig. 1. Surface modification and characterization of UCNPs. (**A**) XRD analysis of UCNPs (NaYF4: Yb: Er = 69%:30%:1%). (**B**) Photos of PAA- and PAH- coated UCNP solutions in PBS solutions. FT-IR (**C**) and thermogravimetric analysis (TGA, **D**) curves of PAH and PAA coated UCNPs. (**E**) Zeta potentials of PAA-UCNPs and PAH- UCNP. (**F**) DLS size distribution of PAA- and PAH-UCNPs.

To determine the stability of the PAA- and PAH- UCNPs in a long time, both of PAA and PAH coated UCNPs were suspended in PBS for one week, followed by size analysis by DLS every day. As shown in Fig. 2A, the sizes of both types of UCNPs remained unmarked changes over the one-week monitoring. TEM analysis of the particle morphology also remained the same as shown in Fig. 2B (TEM morphology immediately after synthesis) and 2C (TEM morphology one week after synthesis) of PAH-UCNPs. The TEM images of PAA-UCNPs also remained unmarked changes within one week (data not shown) . The stability of PAA- and PAH-UCNPs were also analyzed by the fluorescence of the particles after suspended in sterile water for one week. As shown in Fig. 2D (for PAA-UCNPs) and E (for PAH-UCNPs), the intensity of the fluorescence from both types of UCNPs remained unchanged.

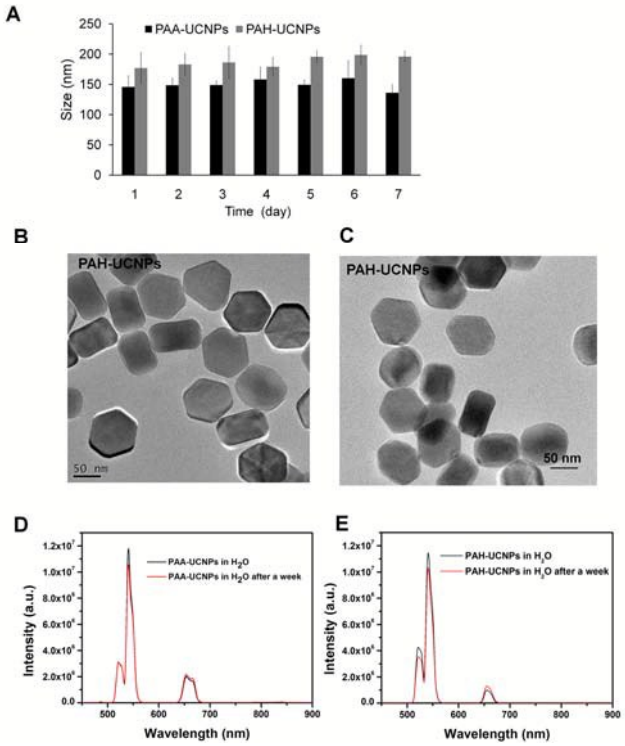

Fig. 2. Stability analysis of PAH- and PAA-modified UCNPs. （A） DLS of the PAH and PAA modified UCNPs. PAH and PAA modified UCNPs were suspended in PBS over a week. The particle sizes were then determined by DLS every 24 h. Morphology analysis of PAH-UCNPs was determined by TEM immediately after synthesis **(B)** or one week after synthesis **(C). (D)** and **(E)** represented the fluorescence intensity before and after suspension in sterile water for one week, respectively.

PAH- but not PAA-modified UCNPs induce autophagy in human blood cancer cells.

UCNPs display great biocompatibility and limited toxicity was reported. As a major response to many chemical, physical, biological stresses, autophagy has been extensively studies in exposure to nanomaterials. But the effect of UCNPs on authophagy is unclear. To this end, we examined whether UCNPs could induce autophagy in blood cancer cells because blood is the first system exposure to these nanomaterials in their biomedical applications. Myeloma (OPM2, JJN3) and leukemia (K562) cell lines were incubated for 9 h at a concentration of 100 μg/mL of PAH- and PAA-UCNPs, respectively. We subsequently examined the protein level of LC3-II, a hallmark of autophagy converted from LC3-I. As shown in Fig. 3A, PAH-UCNPs increased the LC3-II levels in all cells tested but it was not observed in cells exposed to PAA-UCNPs. Notably, PAH-UCNPs-raised LC3-II level was time- and concentration-dependent (Fig. 3B). OPM2 cells were exposed to increased concentrations of PAH-UCNPs for 9 h or 100 μg/mL of PAH-UCNPs for various periods. Immunoblotting revealed that significant LC3-II was observed at a concentration as low as 12.5 μg/mL or in 3 h at the concentration of 100 μg/mL (Fig. 3B). To find out the effects of UCNPs coated with other materials on autophagy in OPM2 cells, four more UCNPs coated with PAA-OA *(octylamine-poly(acrylic acid)*[26], PAA-PEG (polyethylene glycol), OA-PAA-PEI (Polyetherimide), or OA-PAA-PEG, respectively. As shown in Fig.3C, PAH-UCNPs induced the highest level of LC3-II protein as determined by immunoblotting assay. When autophagy is triggered, LC3-II accumulates and form puncta around nucleus. To verify LC3-II expression, OPM2 cells exposed to PAH- or PAA-UCNPs were subjected to immunofluorescent analysis. As expected, starvation resulted in markedly accumulated LC3-II puncta (Fig. 3D). Similar to the treatment of starvation, PAH-UCNPs also led to significant increase of LC3-II dots. However, PAA-UCNPs failed to increase LC3-II puncta in the same treatment (Fig. 3D). All of the above results thus suggested that PAH- but not PAA-modified UCNPs induced autophagy in blood cancer cells.

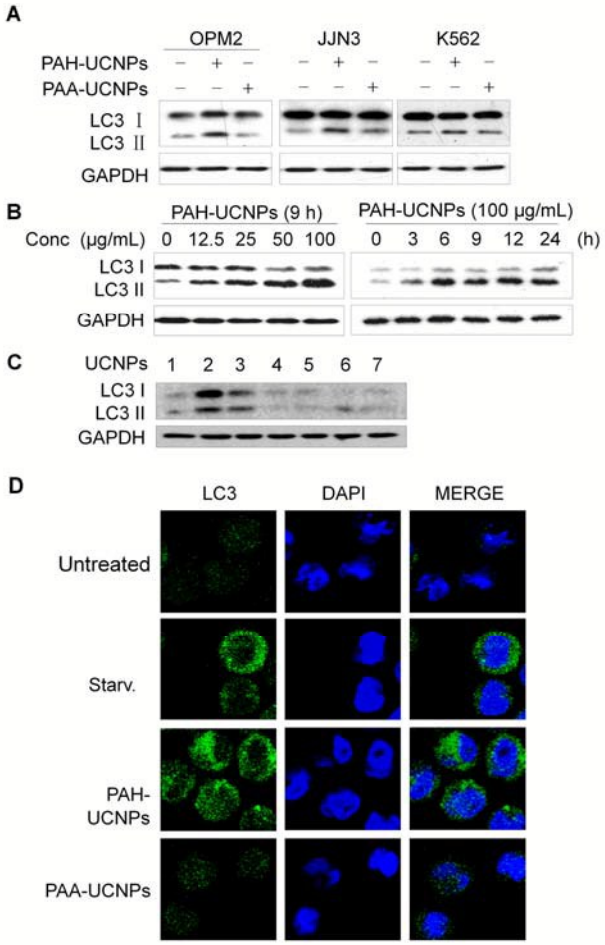

Fig.3. PAH-UCNPs but Not PAA-UCNPs induce autophagy in human blood cells. (**A**) Multiple myeloma (OPM2, 8226) and leukemia (K562) cells were exposed to PAH- or PAA-UCNPs for 9 h at a concentration of 100 μg/mL before analysis. The transformation of LC3-II was analyzed by western blotting using a specific antibody. (**B**) OPM2 cells were incubated with PAH-UCNPs at increased concentrations or extended periods as indicated. Cell lysates were then subject to immunoblotting. (**C**) Six types of UCNPs with different coatings were used to treat OPM2 cells at a concentration of 100 μg/mL for 9 h. Cell lysates were prepared for immunoblotting against LC3-II. 1: Buffer Control; 2: PAH-UCNPs; 3：PAA-UCNPs; 4: OA-PAA-UCNPs; 5: OA-PAA-PEI-UCNPs; 6: PEG-UCNPs; 7: OA-PAA-PEG-UCNPs. (**D**) Immunofluorescent analysis of LC3 puncta. OPM2 cells were treated with PAH- or PAA-UCNPs at a

concentration of 100 μg/mL for 9 h, then stained with specific antibody against LC3-II before being applied to confocal microscopic analysis.

PAH-UCNPs require the PI3KC3/Beclin1/Atg14 complex in autophagy

Autophagy is a multiple-step process involved in several key complexes and signaling transduction. For example, Class III of phosphatidylinositol-3 kinase (PI3KC3) forms a complex with Beclin1/Atg14 to mediate autophagasome formation and elongation, thus it is essential for autophagy. To further understand UCNPs-induced autophagy occurrence, OPM2

were pre-treated with 3-MA, a well known inhibitor of autophagy by targeting PI3KC3, followed by PAH-UCNPs. As shown in Fig.4A, PAH-UCNPs increased LC3-II level, but it was markedly reduced by 3-MA, further suggested that UCNPs-induced autophagy and it was associated with PI3KC3 signaling. Notably, bafilomycin A, an inhibitor of lysosomes, increased LC3-II expression, suggested UCNPs-induced autophagosome is processed in the lysosomes (Fig.4A). These changes demonstrated that PAH-UCNPs could induce autophagy via PI3KC3 in human blood cancer cells and this type of autophagy could be blocked by inhibitors of autophagy or lysosomes.

The above study suggested PI3KC3 was required for UCNPs-induced autophagy. Because PI3KC3 acts in a complex with Atg6/Beclin1 and Atg14, we questioned whether UCNPs interfered with other components of this complex. OPM2 cells were treated with PAH-UCNPs for 9 h at a concentration of 100 μg/mL and then evaluated the expression of associated proteins. Immunoblotting assay revealed that PAH-UCNPs but not PAA-UCNPs induced Beclin1 and decreased Bcl-2 expression (Fig. 4B). PAH-UCNPs induced Beclin1 in a time- and concentration-dependent manner (Fig.4C). In addition to Beclin1, PI3KC3 complex also requires Atg14 in autophagosome formation, therefore, we next measured the effects of PAH-UCNPs on Atg14. It turned out that PAH-UCNPs but not PAA-UCNPs induced the expression of Atg14 (Fig. 4D). All these results above thus suggested PAH-UCNPs induced autophagy by targeting the PI3KC3/Beclin1/Atg14 complex via the induction of Becin1 and Atg14 expression.

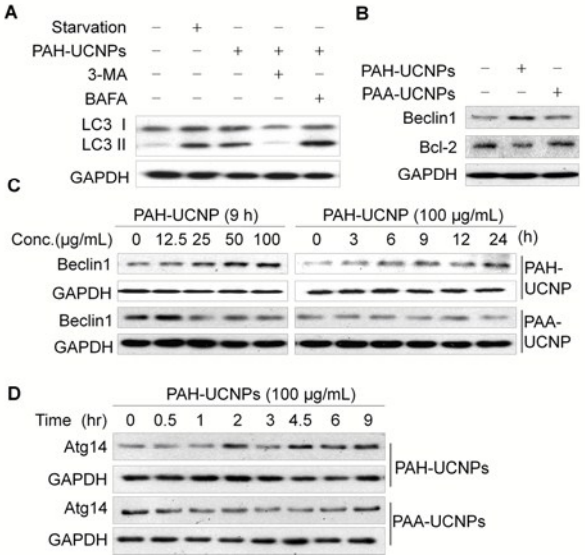

Fig. 4. PAH-UCNPs induce autophagy by affecting the PI3KC3/Beclin1/Atg14 complex. (**A)** OPM2 cells were treated with PPAH-UCNPs alone or with 3-MA or BAFA, followed by evaluation of LC3-II by immunoblotting. Starvation was used as a positive control. **(B)** OPM2 cells were treated with PAH-UCNPs or PAA-UCNPs for 9 h, followed by immunoblotting against Beclin1 or Bcl-2. (**C**) OPM2 cells were treated with PAH-UCNPs at indicated concentrations for 9 h or at 100 μg/mL for indicated periods followed by immunoblotting against Beclin1. (**D**) OPM2 cells were treated with PAH-UCNPs at 100 μg/mL for indicated periods followed by immunoblotting against Atg14.

PAH-UCNPs induce autophagy by targeting Akt/mTOR signaling

The mTOR kinase is believed to be the key player in autophagy initiation, especially in starvation situations. To find out whether PAH-UCNPs also affect mTOR signaling, OPM2 cells were treated with PAH-UCNPs or PAA-UCNPs for 9 h at 100 μg/mL. Immunoblotting showed that PAH-UCNPs but not PAA-UCNPs decreased the protein level of p62, a signature of autophagosome degradation (Fig.5), which was consistent with the previous studies (Figs. 3 and 4). Notably, PAH- but not PAA-coated UCNPs suppressed mTOR phosphorylation. mTOR phosphorylation can be activated by protein kinase B (PKB/AKT) and the later also negatively modulates autophagy [27], we next measured AKT phosphorylation. It turned out that PAH-UCNPs inhibited AKT activation but PAA-UCNPs failed (Fig.5). These results therefore suggested PAH-UCNPs probably induced autophagy initiation by targeting the AKT/mTOR signaling pathway.

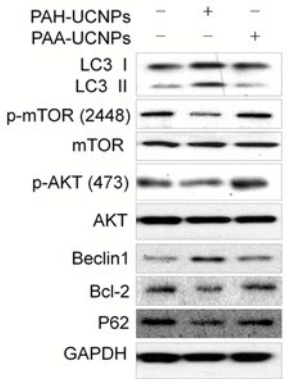

Fig. 5. PAH-UCNPs suppress the AKT/mTOR signaling. OPM2 cells were exposed to PAH-UCNPs or PAA-UCNPs at a concentration of 100 μg/mL for 9 h, followed by immunoblotting against indicated proteins.

PAH-UCNPs induce apoptosis in blood cancer cells

Autophagy has been showed to protect from survival threats in many cells, but more and more studies demonstrated that autophagy also leads to cell death, such as apoptosis [28]. To find out the effects of PAH-UCNPs on final cell fate, we examined apoptotic hallmarks upon UCNP treatment. As shown in Fig.6A, both PARP and caspase-3 were cleaved by PAH-UCNPs, but not affected by PAA-UCNPs. There was more caspase-3 activated with the increase of the concentration of PAH-UCNPs (Fig.6B). These results suggested PAH-UCNPs but not PAA-UCNPs induced myeloma cell apoptosis. To confirm cell apoptosis induced by PAH-UCNPs, OPM2

cells were incubated with PAH- or PAA- UCNPs at increasing concentrations for 24 h, followed by Trypan blue exclusion staining, the results showed that PAH-UCNPs increased dead cells in a concentration-dependent manner, while fewer dead cells were observed in PAA-UCNPs treated cells (Fig. 6C). To find out the effects of these UCNPs on anti-cancer drugs induced apoptosis, three classic anti-myeloma drugs dexamethasone, bortezomib and doxorubicin were used to treated MM cells in the presence or absence of PAH-UCNPs. It showed that PAH-UCNPs enhanced the cleavage of PARP and caspase-3, especially in cells treated with bortezomib (Fig. 6D). However, PAA-UCNPs failed to induce apoptosis or enhance apoptosis in cells treated with bortezomib (Fig.6E). Therefore, the results above indicated that PAH-UCNPs could induce both apoptosis and autophagy, and PAA-UCNPs did not induce apoptosis or autophagy.

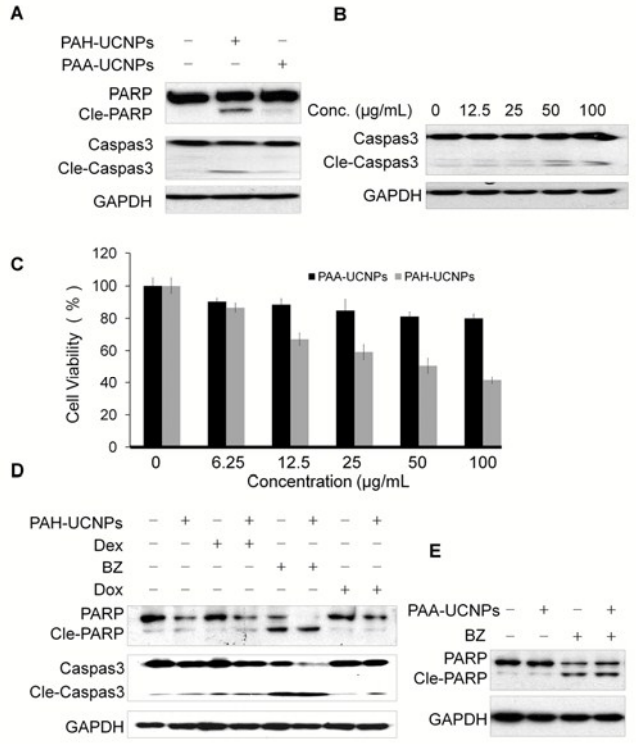

Fig. 6. PAH-UCNPs induce blood cancer cell apoptosis. (**A**) OPM2 cells were treated with PAH-UCNPs or PAA-UCNPs for 9 h at a concentration of 100 μg/mL, followed by the detection of PARP and caspase-3 by immunoblotting assay. (**B**) OPM2 cell lines were exposed to PAH-UCNPs at an increasing concentration for 9 h, caspase-3 activation was detected by immunoblotting. (**C**) OPM2 cells were exposed to PAA- or PAH-UCNPs at indicated concentrations for 24 h, followed by Trypan blue staining assay. (**D**) OPM2 cells were exposed to anti-myeloma drugs Dex, BZ, or Dox in the presence or absence of PAH-UCNPs for 9 h, followed by immunoblotting for the activation of PARP and caspase-3. (**E**) OPM2 cells were treated with PAA-UCNPs and/or BZ, PARP cleavage was detected.

PAH- but not the PAA-coated UCNPs induce autophagy in fresh mice granulocytes

As PAH-UCNPs could induce autophagy in human blood cancer cells, what about the effect on healthy blood cells? To answer this question, granulocytes cells were isolated from healthy mice and then exposed to PAH- and PAA-UCNPs for 9 h at 100 μg/mL. Similar results could also be observed in mice granulocytes. As shown in Fig.7, PAH-UCNPs induced the accumulation of LC3-II and Beclin1, but PAA-UCNPs did not show any effects. These results showed that PAH-UCNPs but not PAA-UCNPs could induce autophagy in mice granulocytes, which was consistent with the effects in blood cancer cells.

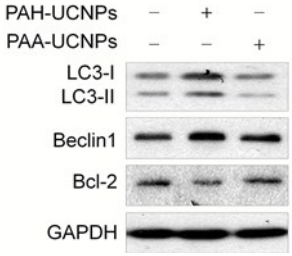

Fig. 7. PAH-UCNPs induce autophagy in fresh mice granulocytes. Myeloid cells were isolated from mice and then exposed to PAH or PAA-UCNPs for 9 h at 100 μg/mL, followed by immunoblotting against Beclin1 and LC3-II.

Both PAA- and PAH- UCNPs are taken up by OPM2 cells

The above results suggested that PAH but not PAA modified UCNPs induced autophagy and apoptosis in blood cells. Because the core structure of these nanoparticles were the same, we wondered whether the coating materials affected the uptake by cells. To determine this point, OPM2 cells were exposed to 0.05 mg of PAA-UCNPs or PAH-UCNPs at 37^{o}C for 0 to 24 h. The concentration of cellular yttrium was determined by ICP-AES. As shown in Fig. 8, yttrium concentrations were increased in both cells treated with PAA- and PAH-UCNPs with the extension of the exposure time, suggesting internalized yttrium element by OPM2 cells were increased over the incubation time. This result implicated that both PAH- and PAA-UCNPs could enter blood cells, but comparatively, PAH coating facilitated the cellular uptake of the UCNPs. These results suggested that the coating materials affected UCNP biological activity in cells.

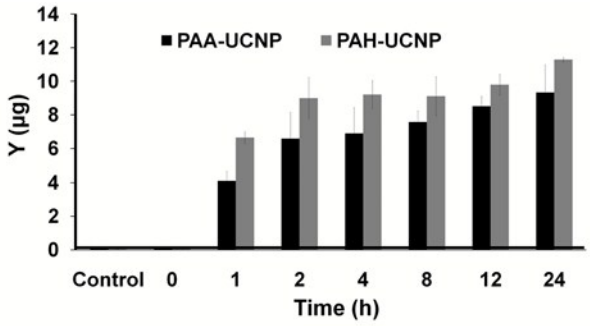

Fig. 8. Internalized yttrium (Y) element by OPM2 cells at different incubation time. OPM2 cells were exposed to the same concentration (0.1 mg) of PAA- or PAH- UCNPs for indicated concentrations. At each time point, cells were collected and washed with PBS for two times before being boiled in aqua regia. Afterwards, the concentration of Y in each sample, which was diluted into 10 mL by water, was measured by ICP-AES.

Discussion

In summary our study showed that PAH-UCNPs induce autophagy in both human and mice blood cells. That PAH-UCNPs induce autophagy in blood cells is supported by (1) the accumulation of LC3 puncta and the LC3-II conversion from LC3-I, a hallmark of autophagy induction, and (2) p62 degradation, a signature of the completeness of the autophagic flux.

Our study also provided potential mechanisms that PAH-UCNPs induce autophagy by targeting AKT/mTOR signaling and the PI3KC3/Beclin1/Atg14 complex, which was confirmed by suppressed p-mTOR and induced Beclin1/Atg14 expression. When PI3KC3 is blocked by 3-MA, a specific inhibitor, PAH-UCNPs-induced autophagy was completely abolished. Moreover, PAH-UCNPs up-regulate the expressions of Beclin1 and Atg14, two essential components in the PI3KC3 complex. As we all know, the Beclin1/Atg14 complex forms the important part in the process of autophagosomes elongation [29]. All findings in the current study demonstrated that the PI3KC3 complex is enhanced by PAH-UCNPs. In addition to PI3KC3, Class I PI3K is also probably involved in PAH-UCNP-induced autophagy. But different from PI3KC3, PI3K forms a cascade signaling transduction, or the PI3K/AKT/mTOR signaling pathway which negatively modulates autophagy. In many cases of autophagy, the PI3K signaling pathway is disrupted which results in suppressed downstream signals such as phosphorylated AKT and mTOR. This holds for PAH-UCNPs because PAH-UCNPs suppressed AKT and mTOR activation. Therefore, PAH-UCNPs probably target both Class I and Class III PI3K signaling, but in a different manner. As demonstrated in this study, PAH-UCNPs increase the Class III PI3K/Beclin1/Atg14 but inhibit PI3K/AKT/mTOR signaling.

Autophagy is believed to represent a protective manner for many cells to avoid further insults from biological, chemical and or physical exposure. For example, in the case of nutrient depletion, autophagy is activated upon AMPK/mTOR signaling. Autophagy can degrade intracellular constituents and damaged cellular organelles to provide cells with nutrients in time [30]. Therefore, autophagy in these cells is cytoprotective. However, in terms of exposure to nanoparticles, the biological effects vary upon individual NPs. In some cases, nanomaterials induce pro-survial autophagy [31]. However, in some cases, autophagy may contribute to cell death. For example, nano-Nd_2O_3 induces cell death in NCI-H460 at a micromolar equivalent [32], while a range of rare earth nanoparticles disrupt autophagic flux [33]. Although photosensitizer-loaded UCNPs have been demonstrated to induce cancer cell death in the presence of therapeutic light irradiation[34, 35], there is no investigation about the direct biological effects of UCNPs on human cells. In the present study, we found PAH-UCNPs directly induce apoptosis in blood cancer cells in addition to autophagy. PARP and caspase-3, the hallmarks of apoptosis, are cleaved and activated by PAH-UCNPs, and this action of PAH-UCNPs can enhance cell death induced by anti-MM drugs such as bortezomib and doxorubicin. However, PAA-modified UCNPs display no induction on either apoptosis or autophagy in the same cells. These two types of UCNPs contain the same chemical core and shell, and the only difference is the surface coating, therefore, the different biological effects in apoptosis and autophagy is probably contributed by the coating materials. PAH or poly-(allylamine hydrochloride) is positively charged, while PAA or poly(acrylic acid) is negatively charged, because cell surface is weakly negatively charged, the positive charge facilitates UCNPs to access cancer cells. This is true for some nanoparticles, for example, polystyrene nanoparticles with different surface modifications display different ability in inducing autophagy in cells [36]. However, our present study showed that both PAA- and PAH- UCNPs could be taken by blood cells although PAH increases the level of UCNPs in cells. We also compared the LC3-II expression by 4 other types of UCNPs modified by negative, positive or neutral polymer coating, it turned out that only PAH-UCNPs significantly raised the autophagy level in the same cells after the same incubation time and incubation concentrations. These results suggest that the negative or positive charge might not be a determinant factor in the activity of the UCNPs, but the coating material itself plays a more important role.

In summary, this is the first study on autophagy and apoptosis directly induced by UCNPs. Because the surface modification attributes to the biological effects of UCNPs, this study suggests it is necessary to take the surface coating into consideration when designing UCNPs for specific biomedical purposes. For example, to enhance the anti-cancer efficacy, PAH-UCNPs are probably an ideal choice, while PAA-UCNPs would be probably better for general diagnostic imaging.

Acknowledgements

This investigation was partly supported by The National Basic Research Program of China (2011CB933501), the Priority Academic Program Development of Jiangsu Higher Education Institutions (PAPD), and by Jiangsu Key Laboratory for Translational Research and Therapeutics of Neuro-Psycho-Diseases (BK2013003). Liang Cheng was supported by the National Natural Science Foundation of China (51302180), a Post-doctoral research program of Jiangsu Province (1202044C) and a Post-doctoral science foundation of China (2013M531400, 2014T70542).

Conflict of Interest

None of the authors has a conflict of interest with this work.

References

1. L. D. Sun, H. Dong, P. Z. Zhang and C. H. Yan, *Annu. Rev. Phys. Chem.*, 2015 **66**,619-42.
2. C. Wang, L. Cheng and Z. Liu, *Theranostics*, 2013, **3**, 317-330.
3. J. Zhou, Z. Liu and F. Li, *Chem. Soc. Rev.*, 2012, **41**, 1323-1349.
4. F. Wang, Y. Han, C. S. Lim, Y. Lu, J. Wang, J. Xu, H. Chen, C. Zhang, M. Hong and X. Liu, *Nature*, 201**0, 463**, 1061-1065.
5. J. Liu, W. Bu, L. Pan and J. Shi, *Angew. Chem. Int. Ed.*, 2013, **52**, 4375-4379.
6. F. Wang, R. Deng, J. Wang, Q. Wang, Y. Han, H. Zhu, X. Chen and X. Liu, *Nat. Materials*, 2011, **10**, 968-973.
7. L. L. Li, R. Zhang, L. Yin, K. Zheng, W. Qin, P. R. Selvin and Y. Lu, *Angew. Chem. Int. Ed.*, 2012, **51**, 6121-6125.
8. L. Cheng, K. Yang, Y. Li, J. Chen, C. Wang, M. Shao, S.-T. Lee and Z. Liu, *Angew. Chem. Int. Ed.*, 2011, **50**, 7385-7390.
9. L.-L. Li, P. Wu, K. Hwang and Y. Lu, *J. Am. Chem. Soc.*, 2013, **135**, 2411-2414.

10. Q. Chen, C. Wang, L. Cheng, W. He, Z. Cheng and Z. Liu, *Biomaterials*, 2014, **35**, 2915-2923.
11. L.-L. Li, R. Zhang, L. Yin, K. Zheng, W. Qin, P. R. Selvin and Y. Lu, *Angew. Chem.*, 2012**, 124**, 6225-6229.
12. R. Li, Z. Ji, J. Dong, C. H. Chang, X. Wang, B. Sun, M. Wang, Y. P. Liao, J. I. Zink, A. E. Nel and T. Xia, *ACS nano*, 2015, 9, 3293-306
13. Z. Li, S. Lv, Y. Wang, S. Chen and Z. Liu, *J. Am. Chem. Soc.*, 2015, 137, 3421-3427.
14. O. S. Wolfbeis, *Chemical Society reviews*, 2015.
15. Z. Zhao, Y. Han, C. Lin, D. Hu, F. Wang, X. Chen, Z. Chen and N. Zheng, *Chem. Asian J.,* 2012, **7**, 830-837.
16. H. Guo, H. Qian, N. M. Idris and Y. Zhang, *Nanomedicine*, 2010, **6**, 486-495.
17. Y. Min, J. Li, F. Liu, E. K. Yeow and B. Xing, *Angew. Chem.*, 2014, **53**, 1012-1016.
18. N. N. Noda and F. Inagaki, *Annu. Rev. Biophy.*, 2015.
19. M. Shi, L. Cheng, Z. Zhang, Z. Liu and X. Mao, *Int. J. Nanomedicine*, 2015, **10,** 207-216.
20. J. Lin, Z. Huang, H. Wu, W. Zhou, P. Jin, P. Wei, Y. Zhang, F. Zheng, J. Zhang, J. Xu, Y. Hu, Y. Wang, Y. Li, N. Gu and L. Wen, *Autophagy*, 2014, **10**, 2006-2020.
21. B. M. Johnson, J. A. Fraietta, D. T. Gracias, J. L. Hope, C. J. Stairiker, P. R. Patel, Y. M. Mueller, M. D. McHugh, L. J. Jablonowski, M. A. Wheatley and P. D. Katsikis, *Nanotoxicology*, 2014, 1-12.
22. S. Hussain and S. Garantziotis, *Autophagy*, 2013, **9**, 101-103.
23. L. Cheng, K. Yang, M. Shao, X. Lu and Z. Liu, *Nanomedicine*, 2011, **6**, 1327-1340.
24. J. Zhang, J. Tang, B. Cao, Z. Zhang, J. Li, A. D. Schimmer, S. He and X. Mao, *PLoS One*, 2013, **8**, e69911.
25. X. Mao, B. Cao, T. E. Wood, R. Hurren, J. Tong, X. Wang, W. Wang, J. Li, Y. Jin, W. Sun, P. A. Spagnuolo, N. MacLean, M. F. Moran, A. Datti, J. Wrana, R. A. Batey and A. D. Schimmer, *Blood*, 2011, **117**, 1986-1997.
26. L. Cheng, K. Yang, S. Zhang, M. Shao, S. Lee and Z. Liu, *Nano Res.*, 2010, **3**, 722-732.
27. D. Heras-Sandoval, J. M. Perez-Rojas, J. Hernandez-Damian and J. Pedraza-Chaverri, *Cellular signalling*, 2014, 26, 2694-2701.
28. Z. F. Chen, Y. B. Li, J. Y. Han, J. Wang, J. J. Yin, J. B. Li and H. Tian, *Autophagy*, 2011, 7, 12-16.
29. Z. Yang and D. J. Klionsky, *Nat. Cell Biol.*, 2010, **12**, 814-822.
30. A. M. Strohecker, J. Y. Guo, G. Karsli-Uzunbas, S. M. Price, G. J. Chen, R. Mathew, M. McMahon and E. White, *Cancer Discov.*, 2013, **3,** 1272-1285.
31. S. T. Stern, P. P. Adiseshaiah and R. M. Crist, *Part. Fibre Toxicol.*, 2012, **9,** 20.
32. M. K. Bakht, M. Sadeghi, S. J. Ahmadi, S. S. Sadjadi and C. Tenreiro, *Nucl. Med. Commun.*, 2013, **34**, 5-12.
33. R. Li, Z. Ji, H. Qin, X. Kang, B. Sun, M. Wang, C. H. Chang, X. Wang, H. Zhang, H. Zou, A. E. Nel and T. Xia, *ACS Nano*, 2014, **8**, 10280-10292.
34. C. Wang, H. Tao, L. Cheng and Z. Liu, *Biomaterials*, 2011, **32**, 6145-6154.
35. N. M. Idris, M. K. Gnanasammandhan, J. Zhang, P. C. Ho, R. Mahendran and Y. Zhang, *Nat. Med.*, 2012, **18**, 1580-1585.
36. C. Loos, T. Syrovets, A. Musyanovych, V. Mailander, K. Landfester and T. Simmet, *Biomaterials*, 2014, **35**, 1944-1953.